

Buffeting Criteria for a Systematic Series of Wings

D. G. Mabey*

Royal Aircraft Establishment, Bedford, England, United Kingdom

In 1970, wind-tunnel measurements were made by NASA of the buffeting on a systematic series of 11 swept wings mounted on top of a simple fuselage. The wings generally had a quarter chord swept 35 deg and an aspect ratio of 6. The emphasis in the original program was on the variation in the onset of buffeting due to wide variations in the wing geometry. In the present paper, approximate criteria for the severity of buffeting have been derived from these measurements. These criteria provide a more complete picture of the effect of variations in wing geometry on the wing buffeting.

Nomenclature

A	= aspect ratio
$C_B(M, \alpha = 0 \text{ deg})$	= buffeting coefficient [Eq. (A1)]
$C_B^*(M, \alpha = 0 \text{ deg})$	= buffeting coefficient [Eqs. (A2) and (A4)]
$C_B^*(M, \alpha)$	= corrected buffeting coefficient [Eq. (A5)]
C_L	= overall lift
f	= frequency
K	= constant [Eq. (A2)]
M	= Mach number
M_{swg}	= rms root-bending moment (in.-lb, Ref. 5)
$\sqrt{nF(n)}$	= tunnel unsteadiness [Eq. (A2)]
q	= kinetic pressure
t/c	= thickness/chord ratio
U	= freestream velocity
α	= wing/body incidence
Λ	= sweep of quarter-chord line
η	= spanwise position (fraction semispan)
ϕ	= leading-edge sweep

Introduction

THE prediction of the boundaries for the onset and severity of buffeting on wings of widely varying designs currently poses an important problem throughout the subsonic and transonic speed ranges. Some limited progress has been made recently to develop a theoretical method for the prediction of buffet onset on swept wings with shock-induced separation bubbles.¹ In addition, both the onset and severity of buffet on a transonic airfoil with periodic flow have been predicted theoretically by Le Balleur and Girodroux-Lavigne.² However, no significant progress has been made to solve the general problem of the prediction of the response of wings to the small-scale, random pressure fluctuations characteristic of buffet excitation.³ The prediction of these small-scale pressure fluctuations probably requires accurate mathematical models of the small-scale turbulence that may not become available for many years.⁴

The verification of new prediction methods for buffeting would be facilitated if an extensive series of reliable buffeting measurements were available for comparison. A recent review suggests that the systematic buffeting measurements on 11 wings made by Ray and Taylor⁵ are still of interest. These measurements illustrate the effects of design variations on the onset of buffeting for wings of moderate/high aspect ratio. However, contours of the severity of buffeting can also be

derived from the measurements (according to a method described previously⁶).

The assumptions required to derive the severity of buffeting are reasonable and well supported by the internal evidence (Appendix A). The contours for light, moderate, and heavy buffeting for four typical wings are given in Appendix B. For some of the wings, regions of exceptionally large responses can be identified, and these are probably due to bistable flows,⁷ some form of aerodynamic resonance, large responses in rigid-body roll, or even "stall flutter." This paper gives the salient conclusions of this review of Ray and Taylor's measurements.

Experimental Details

Model

On the wind-tunnel model, an axially symmetric, steel fuselage was tested in conjunction with 11 steel wings mounted in a high position on the body. This series of models thus provides a simply defined configuration (Fig. 1). Nine of the 11 wings have the quarter-chord line swept 35 deg, but the other two have sweep angles of 25 and 45 deg.

Five of the wings ($\Lambda = 25, 35, \text{ and } 45 \text{ deg}$ with $A = 6$ and $\Lambda = 35 \text{ deg}$ with $A = 4$ and 5) have NACA 63A008 sections. In

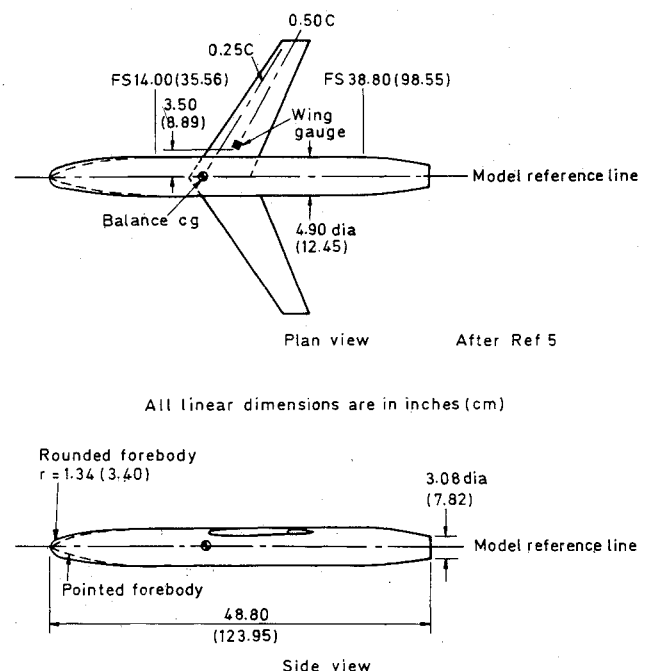


Fig. 1 Sketches of typical model used for buffeting tests.

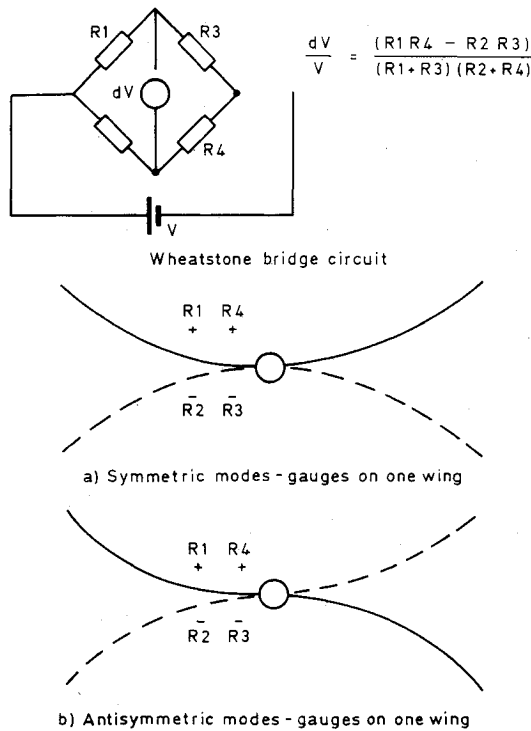


Fig. 2 Signals from wing-root strain bridge.

addition, for $\Lambda = 35$ deg and $A = 6$, there are two cambered wings (with NACA 63A208 and 63A408 sections), two wings with different thickness/chord ratios (with NACA 63A006 and 63A010 sections), and two wings with different positions for the maximum thickness (with NACA 64A008 and 65A008 sections).

Instrumentations and Analysis

Four strain gages were located on each of the starboard wings, so that the bridge responded to both symmetric (Fig. 2a) and antisymmetric motion (Fig. 2b). The total broadband rms signals thus measured (M_{swg} in Figs. 4-24 and term PB-1 in Table 3 of Ref. 5) represent not only symmetric and antisymmetric wing distortion modes, but also rigid-body motion.

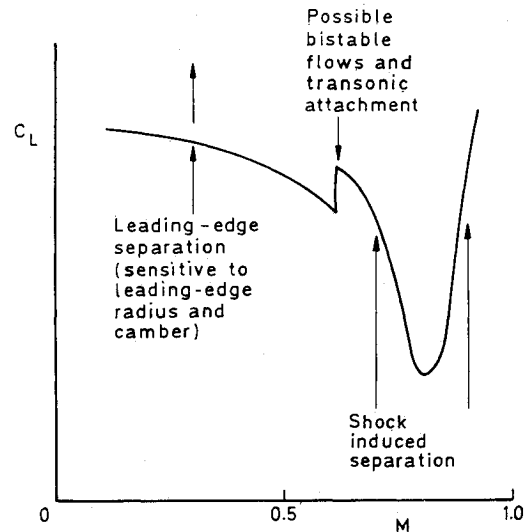
Test Conditions

The measurements were made at low Reynolds number (only about 1.5×10^6 based on a mean chord at $M = 0.6$), but transition was fixed at about 8% chord from the leading edge on both surfaces of the wing, and also on the fuselage. With the section used for seven of the tests (NACA 63A008), scale effects should have been comparatively small with fixed transition.

Results

Typical Variation with Mach Number

Figure 3 shows a typical curve of the lift coefficient for buffet onset, plotted against M . For subsonic speeds (say, $M = 0.2$ to 0.6), this C_L falls slowly as M increases. Usually (for sections of moderate thickness/chord ratio) in this speed range, the separation is initiated at the leading edge (typically at a spanwise position of about $\eta = 0.8$) and occurs at lower values of C_L as M increases, because stronger compressibility effects always increase the adverse pressure gradients in the leading-edge region. In general, configuration changes that increase the leading-edge radius will reduce the adverse pressure gradients and raise the buffet boundary. For low transonic speeds (say, $M = 0.7$ to 0.9), the lift coefficient for buffet onset falls rapidly and then starts to increase. In this speed range, separation is initiated in a complex three-dimensional shock system at about $x/c = 0.5$ and $\eta = 0.8$. Generally, for a fixed incidence, the initial separation moves up-

Fig. 3 Typical variation of C_L for buffet onset with Mach number.

stream and C_L decreases as Mach number increases. However, with a further increase in Mach number, the separation moves downstream and C_L starts to increase. In general, configuration changes that increase three-dimensional effects and weaken the shocks will raise buffet boundaries. In model tests at low Reynolds numbers, the boundary between leading-edge separation and shock-induced separation sometimes gives a bistable flow accompanied by violent buffeting, particularly at low frequencies. There is some evidence in Ref. 5 that bistable flows did occur.

Sometimes buffet onset was masked by the level of flow unsteadiness in the tunnel. It is likely that if the response had been measured in each of the modes, buffet onset would have been defined more precisely for these difficult conditions.

Effects of Sweep ($t/c = 0.08$, $A = 6$)

Figure 4a shows the variation of the C_L for buffet onset with M for sweep angles of 25, 35, and 45 deg. For subsonic speeds, where there is leading-edge separation, increasing sweep lowers the buffet boundary. In contrast, for transonic speeds, increasing sweep raises the buffet boundary, primarily because increasing sweep increases the three-dimensional character of the shock system and thus weakens it (as compared to the equivalent two-dimensional section).

It is found that the buffet onset measurements are not correlated (Fig. 4b) using the expressions appropriate to a swept wing of constant chord and infinite aspect ratio

$$M_n = M \cos \phi \quad (1)$$

$$C_{Ln} = C_L s^2 \phi \quad (2)$$

Primarily, this is because as the sweep increases, the effective thickness/chord ratio and leading-edge radius on sections normal to the leading edge also increase. Thus, at subsonic speeds and constant M_n , increasing ϕ increases the effective leading-edge radius and therefore raises the buffet boundary. Similarly, at transonic speeds and constant M_n , increasing ϕ increases the effective thickness/chord ratio and enhances the effects of shock-induced separation, lowering the buffet boundary.

Some general remarks about the severity of buffeting are appropriate. The contours for moderate buffeting are virtually unchanged for $\Lambda = 25$ and 35 deg (Figs. 4a and 4c). However, for $\Lambda = 45$ deg, the moderate buffeting contour is appreciably higher at Mach numbers above 0.4, reflecting the development of a swept, highly three-dimensional bubble (Fig. 4c).

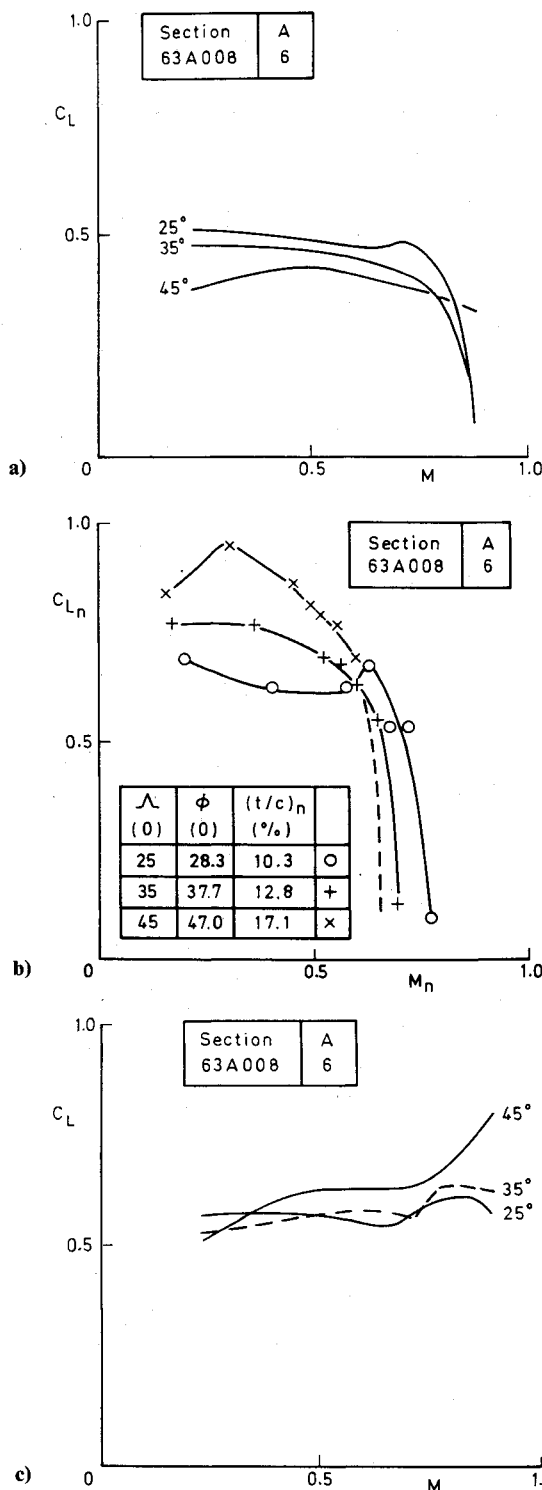


Fig. 4 Effect of sweep on buffeting: a) onset; b) attempt to correlate onset for wings of varying sweep; c) moderate.

Effect of Camber ($\Lambda = 35$ deg, $t/c = 0.08$, $A = 6$)

For subsonic speeds, positive camber raises the buffet boundary significantly (Fig. 5a). This is because increasing the camber reduces the adverse pressure gradients in the leading-edge region and therefore delays the onset of leading-edge separation. For transonic speeds, the development of the three-dimensional flow is sensitive to the planform and section selected, and no general trend can be identified.

It is remarkable that at both subsonic and transonic speeds, positive camber also increases the lift coefficient for moderate buffeting. This is the largest benefit achieved by the design variations tested (Fig. 5b).

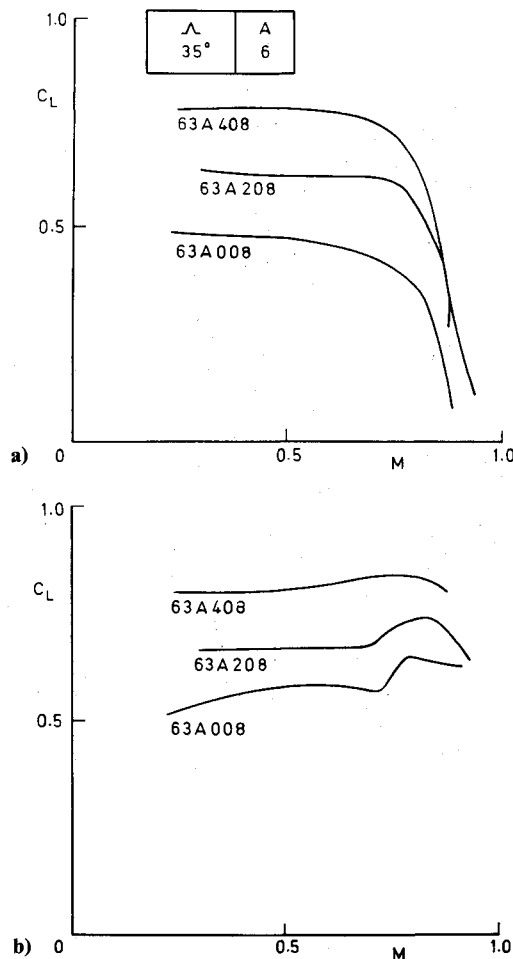


Fig. 5 Effect of camber on buffeting: a) onset; b) moderate.

Effect of Thickness/Chord Ratio ($\Lambda = 35$ deg, $A = 6$)

For subsonic speeds, increases in the thickness/chord ratio raise the buffet boundary (Fig. 6a). This is because as t/c increases (for a given section), the leading-edge radius increases and, thus, reduces the adverse pressure gradients around the leading edge. Thus, leading-edge separation is delayed. In contrast, for transonic speeds, increases in t/c generally lower the buffet boundary, because the shocks are strengthened and separation occurs earlier. The advantage for the thinnest section is large, particularly at $M = 0.85$.

For the moderate buffeting contours, no clear trends can be inferred at subsonic speeds (Fig. 6b). However, there is a suggestion that the severity of buffeting will be higher with the thicker sections at transonic speeds, consistent with experience on airfoils.

Effect of Position of Maximum Thickness ($\Lambda = 35$ deg, $t/c = 0.08$, $A = 6$)

For a given thickness/chord ratio, a significant effect of moving the maximum thickness aft is to decrease the leading-edge radius. Therefore, for subsonic speeds, moving the position of maximum thickness aft lowers the buffet boundary (Fig. 7a). For transonic speeds the development of the three-dimensional wing flow is more difficult to assess, and no universal trend can be identified. Possibly, the predominant effect of the downstream movement of maximum thickness is a general downstream movement of the sonic line. This would limit the extent of local supersonic flow, weaken the shock systems, and raise the buffet boundary. Certainly, for this wing at transonic speeds, moving the maximum thickness aft from $x/c = 0.30$ to 0.50 raises the buffet boundary. (Moving the position of maximum thickness even further downstream

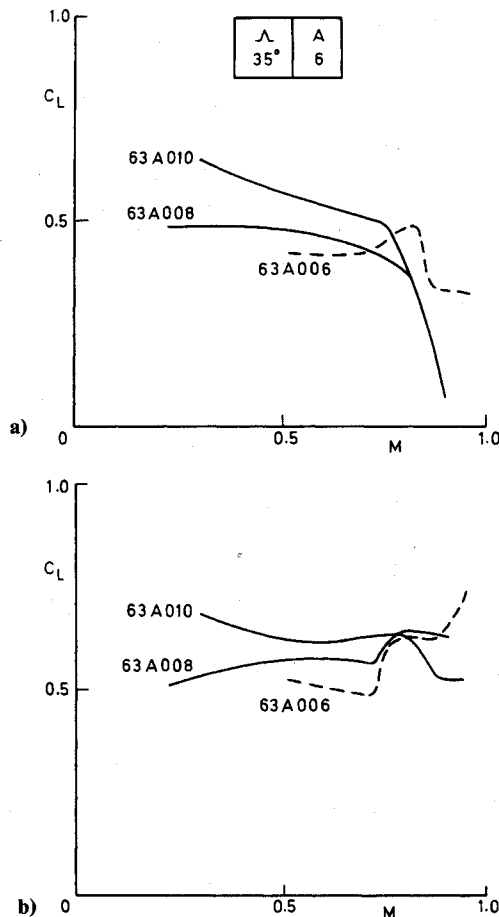


Fig. 6 Effect of thickness/chord ratio on buffeting. : a) onset; b) moderate.

should ultimately increase the adverse pressure gradient between the shock and the trailing edge. Then separation would occur at lower angles of incidence, so that the buffet boundary would be lowered.)

For moderate buffeting contours (Fig. 7b), no clear trend is suggested.

Effect of Aspect Ratio ($\Lambda = 35$ deg, $t/c = 0.08$)

For subsonic speeds, the present measurements show that the buffet boundary is raised as the aspect ratio increases. In contrast, for transonic speeds, the buffet boundary is lowered as the aspect ratio increases (Fig. 8a). This is because as aspect ratio increases, the shock system tends toward the limit of that of an infinite swept wing, which is quasi-two-dimensional. In the limit, as aspect ratio tends to infinity, a series of lambda shock waves of varying strength (viewed on the planform) is replaced by a single, much stronger shock of constant strength, which lowers the buffet boundary. For the moderate buffeting contour, no clear trend is suggested (Fig. 8b).

Attempts to Infer Buffet Onset from Steady-Force Measurements

After a careful review of the six-component measurements, Ray and Taylor concluded⁵ that derivation of buffet onset from steady measurements was virtually impossible. In particular, the often used "clue" of the initial break in the C_L vs α curve could occur well above or even below buffet onset (for a wing of low sweep). However, they suggested that a comparison of measured and predicted C_A vs α curves (e.g., Fig. 4b of Ref. 5) and its association with leading-edge suction could sometimes be used to confirm the incidence for buffet onset, where this was masked by the response to flow unsteadiness.

Some early unpublished Royal Aircraft Establishment (RAE) tests on a wing swept 25 deg had suggested that there might be a correlation between the minimum in the $C_A - \alpha$

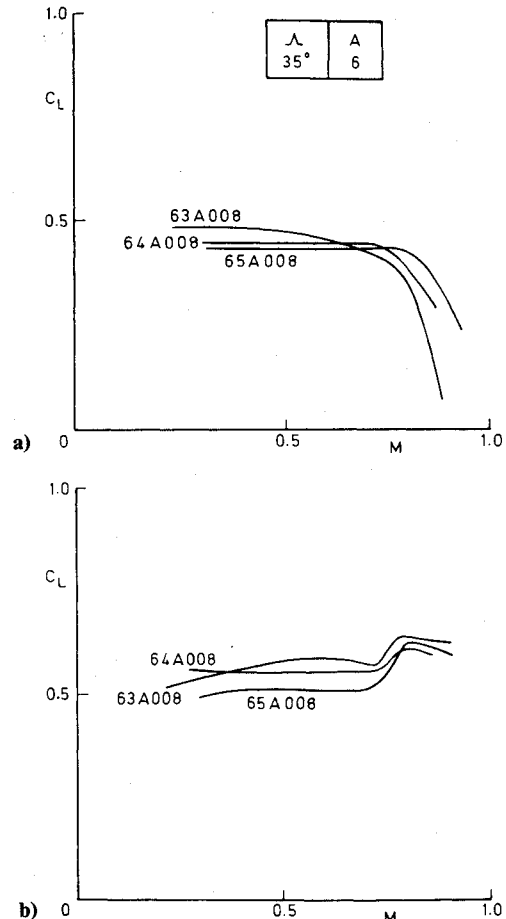


Fig. 7 Effect of position of maximum thickness on buffeting. : a) onset; b) moderate.

curve and the moderate buffeting level. A comparison of the observed minima in the axial force curves⁵ and the present contours for moderate buffeting does not always support this correlation. Ray suggests that correlations of this type exist for thick wings of low sweep, with leading-edge, bubble-type separations. In contrast, no such correlations exist for thin, highly swept wings where there are leading-edge vortices. Ray et al.¹² also demonstrated¹² the effectiveness of leading-edge and trailing-edge flaps, or variable camber, in raising buffet onset on the basic model of Ref. 5 (wing 2).

Discussion

After a careful analysis of the measurements of Ref. 5, some interesting effects of design changes on wing buffeting have been illustrated in Figs. 4-8. The measurements for the onset of buffeting are taken directly from Fig. 25 of Ref. 5, but the criterion for moderate buffeting is derived as described in Ref. 6 and Appendix A.

The choice of the moderate buffeting criterion as an indicator of design changes needs some explanation. Few transport aircraft ever exceed the light buffeting limit⁶; this would have been the natural choice for wings of 35 deg sweep and aspect ratio 6. However, such a choice would have had two disadvantages:

- 1) For many conditions, the difference between buffet onset and light buffeting would have been too small to be significant, even with the correct value of K (Appendix A).

- 2) The criterion chosen should allow for the possibility of an error in the choice of K . If the actual level of tunnel unsteadiness was higher [say, $\sqrt{nF(n)} = 0.0030$, instead of the value 0.0015 selected], then K would be twice as big. The moderate buffeting levels shown here would then correspond to heavy buffeting.

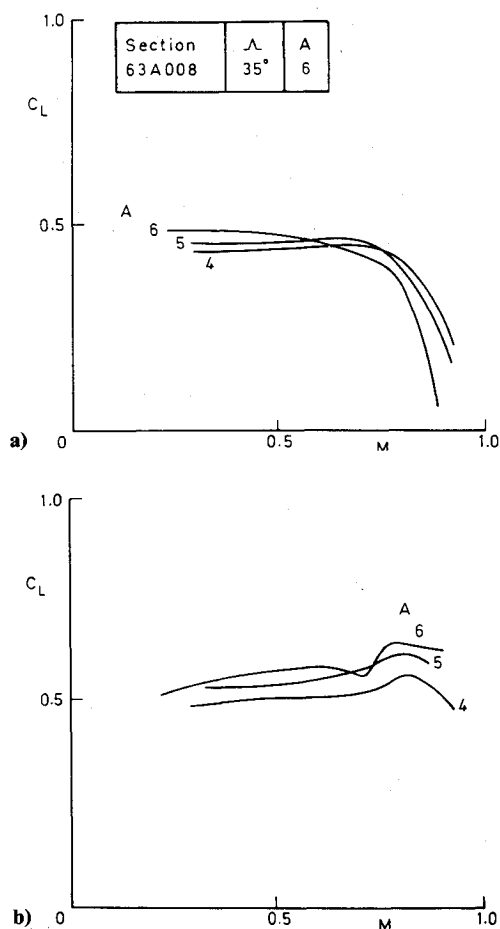


Fig. 8 Effect of aspect ratio on buffeting: a) onset; b) moderate.

There is independent evidence from other wind-tunnel tests⁸ that the 'level of flow unsteadiness in the NASA Langley 7×10 ft tunnel is indeed closer to $\sqrt{nF(n)} = 0.0015$ than to 0.0030 or 0.00075. In Ref. 8, extensive measurements of wing buffeting were made on an ordinary wind-tunnel model of the Phantom aircraft. From the typical buffeting measurements presented at $M = 0.80$ (Ref. 8, Fig. 3), a level of about $\sqrt{nF(n)} = 0.0020$ can be inferred from the well-defined maximum buffeting response (equivalent to $C_B^* = 0.016$) and the response at low angles of incidence due to flow unsteadiness. However, this level of flow unsteadiness occurs at a first wing-bending frequency of 155 Hz. Measurements in the closed working section of the RAE 8×8 ft tunnel⁹ suggest that some reduction in flow unsteadiness would occur from 155 Hz to the present first wing-bending frequency (estimated at about 70 Hz), and it does not seem unreasonable that a similar reduction should occur in the NASA Langley 7×10 ft tunnel. Therefore, the choice of

$$\sqrt{nF(n)} = 0.0015 \quad (3)$$

appears appropriate.

Thus, it is considered that reliable criteria for both the onset of buffeting and moderate buffeting can be derived from the measurements of Ref. 5, which relate to a simple configuration a wing of 35 deg sweep and an aspect ratio of 6. For civil aircraft with this sweep, interest would be centered now on much higher aspect ratios (say, 10 to 12), whereas for military aircraft, much lower aspect ratios (say, 2 to 4) would be of interest. However, systematic buffeting measurements of this type are unlikely to be made again.

The levels of light, moderate, and heavy buffeting, derived according to the semiempirical buffeting coefficients C_B^* of Ref. 6, should correspond to the absolute coefficients for the

buffet excitation parameter $\sqrt{nG(n)}$, derived according to Ref. 10.

Finally, it should be noted that these measurements included no variation with Reynolds number at constant Mach number, although they were made with fixed transition. It is hoped that buffeting measurements over a much wider range of Reynolds number will become available soon from tests of widely different aircraft configurations in the cryogenic National Transonic Facility at NASA Langley. These measurements should provide an indication of the magnitude of scale effects on both the onset of buffeting and the severity of buffeting.

Concluding Remarks

After a reanalysis of the measurements of Ref. 5, criteria for light, moderate, and heavy buffeting have been derived for a systematic series of 11 wings. The effects of the principal design variations on the wing buffeting are illustrated in graphs in the $C_L - M$ domain, giving the contours for the onset of buffeting (reproduced directly from Ref. 5) and moderate buffeting. For subsonic speeds, where buffeting is due to a leading-edge separation, most of the variations are caused by changes in the leading-edge radius.

The effects of the five principal design variations are now enumerated.

1) Increasing the leading-edge sweep from 25 to 45 deg lowers the boundary for the onset of buffeting at subsonic speeds but raises it at transonic speeds. The boundary for moderate buffeting is raised as sweep increases.

2) Increasing camber raises the boundaries for both onset and moderate buffeting at subsonic speeds, but there is no general trend for transonic speeds.

3) Increasing the thickness/chord ratio raises both the onset and moderate buffeting boundaries at subsonic speeds, but no clear trend is apparent at transonic speeds.

4) At subsonic speeds, moving the position of maximum thickness aft lowers the boundaries for both onset and moderate buffeting at subsonic speeds. For transonic speeds, moving the position of maximum thickness aft raises the buffet onset boundary without establishing a clear effect on the boundary for moderate buffeting.

5) At subsonic speeds, increasing the aspect ratio raises the boundaries for both the onset of buffeting and moderate buffeting. Increasing the aspect ratio at transonic speeds lowers the boundary for the onset of buffeting but raises the moderate buffeting contour.

In addition to these specific conclusions, very high levels of buffeting coefficient ($C_B^* > 0.032$) have been identified in certain areas for 10 of the 11 wings tested. In these regions, there are probably bistable flows, some form of aerodynamic resonance, a large response in the rigid-body roll mode, or possibly stall flutter. Such regions would be of equal interest with respect to aircraft handling (wing drop and wing rocking problems) as for wing buffeting.

Appendix A: Choice of Relationship Between the Wing Response and the Assumed Flow Unsteadiness

The semiempirical method developed in Ref. 6 applies solely to buffeting in the first wing-bending mode. It is assumed that for these tests, the measured unsteady wing-root strain signal (quoted in Ref. 5 as M_{swg} in Figs. 4-24 and the term PB-1 in Table 3) represents the response solely in the first wing-bending mode. This assumption is likely to be valid only for light/moderate levels of buffeting, in which experience on other models suggests¹⁰ that there is generally no significant response in antisymmetric modes or in the rigid-body roll mode. For heavy levels of buffeting, there may well be a significant response in these unwanted modes, and for very heavy levels of buffeting, low-frequency modes or stall flutter may predominate. If these unwanted modes are excited, they will contribute to the wing-root strain signal because the strain

gages were all on the starboard wing in the tests⁵ (see Figs. 1 and 2). Hence, contours for heavy buffeting derived on the assumption that all the response is in the first wing symmetric-bending mode will be in error. (See discussion of Fig. 10 in Appendix B.)

Following the notation of Ref. 6, we define a coefficient C_B ($M, \alpha = 0$ deg) such that

$$C_B(M, \alpha = 0 \text{ deg}) = \frac{\text{wing-root strain signal at zero incidence}}{\text{kinetic pressure}} \quad (A1)$$

$$= (M_{\text{swg}})_{\alpha = 0 \text{ deg}}/q$$

This coefficient represents the response of the wing under attached flow conditions to the flow unsteadiness in the wind tunnel, which should be constant over the incidence range for which the flow is attached. A relationship is now sought between $C_B(M, \alpha = 0 \text{ deg})$ and the level of flow unsteadiness in the wind tunnel $\sqrt{nF(n)}$ as defined in Refs. 3, 9 and 11. This relationship is

$$C'_B(M, \alpha = 0 \text{ deg}) = \sqrt{nF(n)} = KC_B(M, \alpha = 0 \text{ deg}) \quad (A2)$$

where K is determined from the root-strain measurements and Eq. (3).

Table A1 includes a column indicating how the variations in K might be associated with variations in wing frequency, but these variations could be due to variations in structural damping. Seven of the 11 wings have the same value of K ; hence, for these wings, comparison of measurements of buffeting should be particularly reliable.

The values of K given in Table A1 are applied to all the other buffeting measurements in Ref. 5 for the combinations of M ,

α available to form coefficients

$$C'_B(M, \alpha) = KC_B(M, \alpha) \quad (A3)$$

The final stage in the derivation of the wing buffeting contours is the removal of the tare response due to flow unsteadiness, $C'_B(M, \alpha = 0 \text{ deg})$, from the total response, $C'_B(M, \alpha)$. If the tunnel response and the model buffeting are uncorrelated,

$$C''_B(M, \alpha) = \sqrt{C'_B(M, \alpha)^2 - C'_B(M, \alpha = 0 \text{ deg})^2} \quad (A4)$$

Equations (A1-A4) have been applied to derive the buffeting contours shown in Fig. 9 and discussed briefly in Appendix B. Units of K in Eq. (A2) are $q/M_{\text{swg}} = (\text{lb}/\text{ft}^2)/\text{in.}\cdot\text{lb}$ to allow direct use of Table 3 in Ref. 5, despite inconsistency of units.

Table A1 Values of K

Wing	K	Note on variations in wing frequency
1	0.103	Only a small change with sweep, despite variation in thickness normal to leading edge.
2	0.103	
3	0.103	
4	0.124	Big change due to thin section.
5	0.077	Big change due to thick section.
6	0.103	Only a small change due to variation in position of maximum thickness.
7	0.103	Only a small change due to camber.
8	0.103	Apparently larger change due to camber.
9	0.077	Only a small change due to aspect-ratio variation.
10	0.103	Only a small change due to aspect-ratio variation.
11	0.077	Apparently larger change due to aspect-ratio variation.

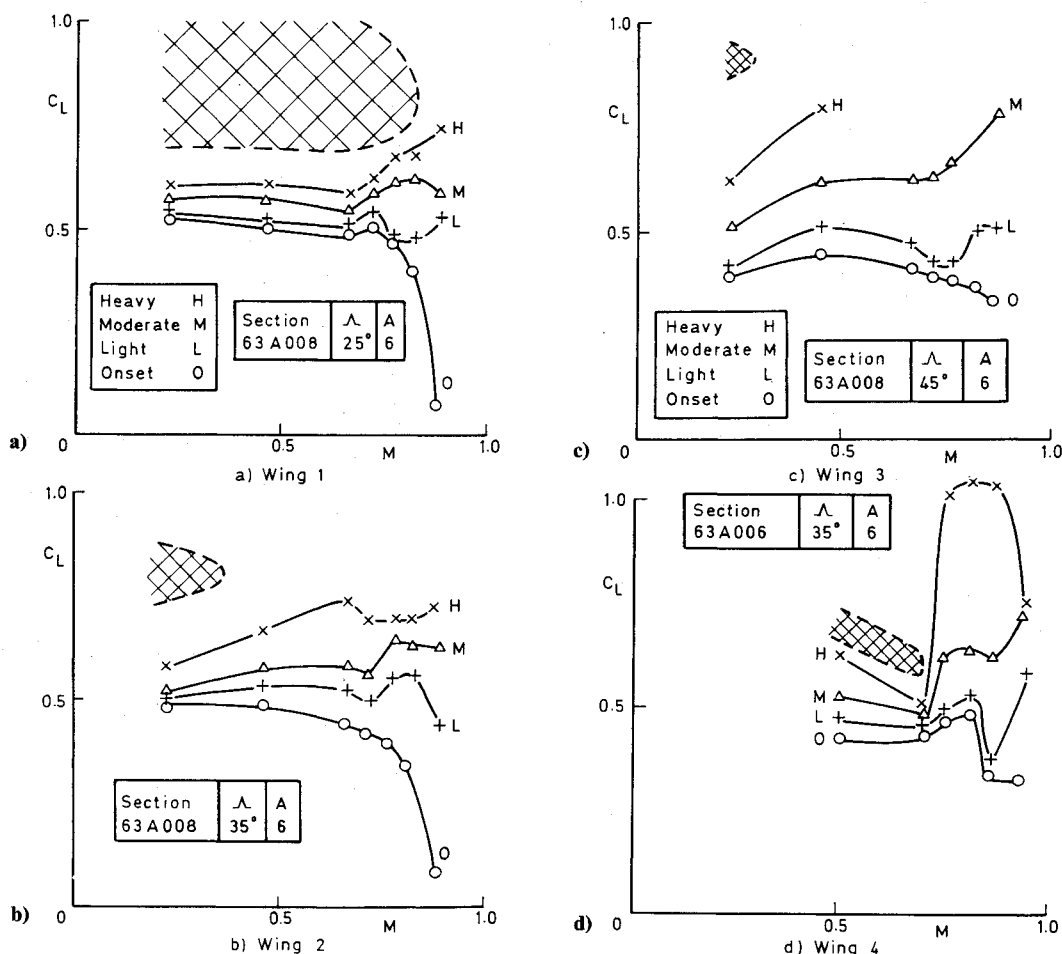


Fig. B1 Contours of buffeting: a) wing 1; b) wing 2; c) wing 3; d) wing 4.

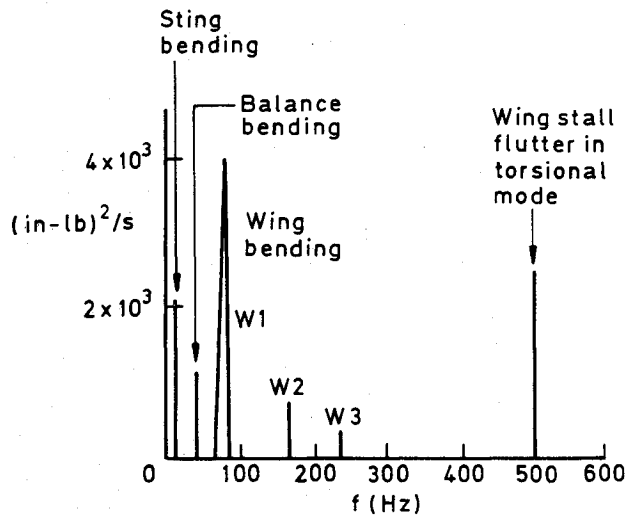


Fig. B2 Power spectrum of wing-root strain signal: Wing 4, $M = 0.503$, $C_L = 0.6$. (Courtesy of E. J. Ray, unpublished.)

Appendix B: Notes on Buffeting Contours for Wings 1 to 4

Figure B1 shows buffeting contours for wings 1 to 4, drawn in the C_L domain according to the criteria of Ref. 6: Onset of buffeting, $C_B'' = 0$; light buffeting, $C_B'' = 0.004$; moderate buffeting, $C_B'' = 0.008$; heavy buffeting, $C_B'' = 0.016$. In addition, a new category, very heavy buffeting, $C_B'' > 0.032$, is introduced. These areas are shown shaded in the $C_L - M$ domain. These high buffeting coefficients may be due to bistable flows, some form of aerodynamic resonance, stall flutter, or large responses in antisymmetric modes, in particular in the rigid-body roll mode. These shaded areas would deserve special attention in any study of aircraft handling characteristics. Contours for wings 5 to 11 are available also,¹³ but are omitted here for the sake of brevity.

Wing 1 ($\Lambda = 25$ deg, Fig. B1a)

The buffeting contours are fairly closely spaced at subsonic speeds but are much more widely spaced at transonic speeds: this is a characteristic typical of many other wings. For the Mach number range $0.2 < M < 0.7$ and $0.7 < C_L < 1.0$, there is a large area with very heavy buffeting.

Wing 2 ($\Lambda = 35$ deg, Fig. B1b)

The buffeting contours generally are more widely spaced at subsonic speeds than for wing 1, indicating a strong favorable effect of sweep on the increase in the severity of buffeting. The area of very heavy buffeting for wing 2 is restricted to $M = 0.2$ and $0.73 < C_L < 0.87$, i.e., greatly reduced relative to wing 1.

Wing 3 ($\Lambda = 45$ deg, Fig. B1c)

The buffeting contours are even more widely spaced at subsonic speeds than for wing 2, indicative of a further favorable effect of sweep. Within the test range, the heavy buffeting limit is not reached above about $M = 0.50$. Very heavy buffet-

ing at $M = 0.2$ is restricted to a narrow range in C_L (about 0.85 to 0.95).

Wing 4 ($\Lambda = 35$ deg, NACA 63A006 Section, Fig. B1d)

The buffeting contours suggest a sudden change from a leading edge to a shock-induced separation at about $M = 0.70$. In the Mach number range from $M = 0.5$ to 0.7 , there is a tongue-shaped region of very heavy buffeting that may be caused by some form of bistable flow or stall flutter. For wing 4 alone, a power spectrum of the wing-root strain signal exists for $M = 0.503$ at a C_L of 0.6 and is reproduced in Fig. B2. The spectrum shows the largest power in the first wing-bending mode, but with significant power in a stall flutter mode and much smaller powers in sting- and balance-bending modes. This condition corresponds to the heavy buffeting limit ($C_B'' = 0.016$) in Fig. B1d, which must accordingly be in error.

Acknowledgment

The author would like to thank Ed Ray of NASA Langley for permission to reproduce some hitherto unpublished buffeting measurements on wing 4 (Fig. B2) and for his comments on the draft of this paper.

References

- ¹Fulker, J. L. and Ashill, P. R., "A Model of the Flow over Swept Wings with Shock Induced Separation," *IUTAM Symposium on Turbulent Shear-Layer/Shock Wave Interactions*, Springer-Verlag, New York, 1985, pp. 233-245.
- ²Le Balleur, V. C. and Girodroux-Lavigne, P., "Prediction of Buffeting and Calculation of Unsteady Boundary-Layer Separation on Aerofoils," *IUTAM Symposium on Boundary-Layer Separation*, Springer-Verlag, New York, 1987.
- ³Mabey, D. G., "Beyond the Buffet Boundary," *Aeronautical Journal*, No. 748, April 1977, pp. 201-215.
- ⁴Chapman, D. R., "Computational Aerodynamics: Development and Outlook," *AIJA Journal*, Vol. 17, Dec. 1979, pp. 1293-1313.
- ⁵Ray, E. J. and Taylor, R. T., "Buffet and Static Aerodynamic Characteristics of a Systematic Series of Wind Tunnel Study," NASA TND 5805, 1970.
- ⁶Mabey, D. G., "A Hypothesis for the Prediction of Flight Penetration of Wing Buffeting from Dynamic Tests on Wind Tunnel Models," Aeronautical Research Council, CP 1171, 1971.
- ⁷Mabey, D. G., Welsh, B. L., and Pyne, C. R., "Effects of Boundary Layer Fences on Canard Control Power and Buffeting," Royal Aircraft Establishment, Bedford, England, RAE Tech. Memo. Aero 2097, 1987.
- ⁸Hollingsworth, E. G. and Cohen, M., "Comparison of Wind Tunnel and Flight Test Techniques for Determining Transonic Buffet Characteristics on the McDonnell Douglas F-4 Airplane," AIAA Paper 70-584, 1970.
- ⁹Mabey, D. G., "Flow Unsteadiness and Model Vibration in Wind Tunnels at Subsonic and Transonic Speeds," CP 1155, 1971.
- ¹⁰Mabey, D. G. and Cripps, B. E., "Some Measurements of Buffeting on a Flutter Model of a Typical Strike Aircraft," AGARD CP 339, Paper 13, 1982.
- ¹¹Mabey, D. G., "Some Remarks on the Design of Transonic Tunnels with Low Levels of Flow Unsteadiness," NASA CR 2722, 1976.
- ¹²Ray, E. J., McKinney, L. W., and Carmichael, J. G., "Maneuver and Buffet Characteristics of Fighter Aircraft," NASA TND 7131, 1973.
- ¹³Mabey, D. G., "Criteria for the Onset and Severity of Buffeting on a Systematic Series of Eleven Wings," Royal Aircraft Establishment, Bedford, England, RAE Tech. Memo. Aero 2103, 1987.